AN IMPROVED UNITARIZATION METHOD AND A SEARCH FOR MOLECULAR-TYPE HIDDEN-CHARM PENTAQUARKS*

V.K. Magas, E.E. Garcia Gonzales, A. Ramos

Departament de Física Quàntica i Astrofísica
& Institut de Ciències del Cosmos (ICCUB), Universitat de Barcelona
Martí i Franquès 1, 08028 Barcelona, Spain

Received 30 April 2026, accepted 13 May 2026,
published online 10 July 2026

We study hidden-charm pentaquarks dynamically generated in meson–baryon interactions. The corresponding scattering amplitude is unitarized via the Bethe–Salpeter equation within an improved method, where the meson–baryon loop function is regularized in a new hybrid scheme. This scheme automatically avoids the generation of unphysical poles, typical for cut-off or dimensional regularizations, while keeping the masses of the physical poles unchanged. Moreover, this improved scheme allows us to make new predictions in the $S = -1, I = 1$ sector.

DOI:10.5506/APhysPolBSupp.19.4-A14

1. Introduction

The existence of pentaquark resonances $P_{c\bar{c}}(4312)^+$, $P_{c\bar{c}}(4380)^+$, $P_{c\bar{c}}(4440)^+$, $P_{c\bar{c}}(4457)^+$, $P_{c\bar{c}s}(4338)^0$, and $P_{c\bar{c}s}(4459)^0$, established by the LHCb Collaboration [1–5], has been one of the major discoveries in hadron physics in recent years. Most of these states, except $P_{c\bar{c}}(4380)^+$, due to its large width $\Gamma = 210 \pm 90$ MeV [1], can be understood as meson–baryon bound states. To describe these exotic baryons as hadronic molecules, theoretical frameworks have been developed that seek to expand the SU(3) flavor symmetry to include heavy quarks in meson–baryon interactions. The model derived in [6] employs the local hidden gauge approach (LHGA) assuming SU(4) flavor symmetry (hereafter referred to as LHGA-SU(4)), while the model derived in [7] is also based on the LHGA but explicitly uses baryon flavor wave functions without assuming SU(4) symmetry (hereafter referred to as LHGA-WF).

* Presented by V.K. Magas the Excited QCD 2026 Workshop, Granada, Spain, 8–14 January, 2026.

More recently, further studies have been carried out on hidden-charm pentaquarks with strangeness $S = -2$ [8–10], and new possible states were predicted. The authors of Refs. [8, 10] employed the LHGA-SU(4) model, and the authors of Ref. [9] reanalyzed the same sector using the LHGA-WF method. The main difference between the two approaches lies in the widths of the states; those from the LHGA-WF method are narrower, which stems clearly from the differences in the kernel coefficients. While the diagonal coefficients in the LHGA-SU(4) and LHGA-WF models are exactly the same, there are some differences in the off-diagonal coefficients responsible for available decay modes.

These double-strange molecular-type pentaquarks are dynamically generated in a very specific way via a strong non-diagonal attraction between the two heaviest meson–baryon channels [8]. They were overlooked in earlier similar studies, such as [11], because other research groups were discouraged by the repulsive character of the diagonal kernel coefficients, and because the complex structure of the resulting scattering amplitudes — dominated by unphysical structures — obscured these physical states. This motivated us to develop an improved unitarization scheme that avoids the appearance of unphysical poles.

As we will show below, our new algorithm indeed leads to a much cleaner output for the scattering amplitude, maintaining all physical poles at practically the same positions and avoiding the generation of fake poles. Furthermore, our preliminary results have already allowed us to find more poles in the $S = -1$, $I = 1$ sector, which were also overlooked in previous studies, most probably for the same reason.

2. Formalism and an improved unitarization scheme

Our model relies on a meson–baryon interaction in S-wave, built from the t-channel diagram shown in Fig. 1. We shall focus on the interaction of pseudoscalar mesons with $(1/2^+)$ baryons (PB interaction). However, we would like to stress that the model for vector meson interactions with the same baryons (VB interaction) is very similar; thus, each state found in the PB sector has an analog in the VB sector.

The VPP and VBB vertices in the diagram are described by effective Lagrangians obtained using the local hidden gauge formalism and assuming SU(4) symmetry. In the limit where the mass of the exchanged meson is much larger than its four-momentum, the t-channel diagram of Fig. 1 reduces to a contact term, and its S-wave expression reads

$$V_{ij}(\sqrt{s}) = -C_{ij}\frac{1}{4f^2}\left(2\sqrt{s} - M_i - M_j\right) N_i N_j \,, \tag{1}$$

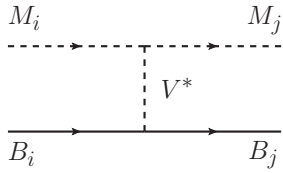

Fig. 1. Leading-order tree-level diagram contributing to the meson–baryon interaction. Baryons and mesons are depicted by solid and dashed lines, respectively; indices i, j label the different meson–baryon channels with the same spin-parity, isospin, and flavor quantum numbers that can be connected by the exchange of a vector meson V^*.

where N_i and N_j are normalization factors, $N_i = \sqrt{(E_i + M_i)/2M_i}$, while M_i (E_i) and M_j (E_j) are the mass (energy) of the baryon in the incoming and outgoing channels, respectively. The coefficients C_{ij} contain the SU(4) Clebsch–Gordan factors encoded in the Lagrangians, as well as the ratio between a characteristic mass of the light uncharmed vector meson and the mass of the actual vector meson exchanged. Further details of the formalism can be found in Ref. [12].

In order to find a properly unitarized scattering amplitude, T_{ij}, we employ the Bethe–Salpeter equation in coupled channels, which implements a resummation of meson–baryon loops, G_l, to infinite order

$$T_{ij} = V_{ij} + V_{il} G_l T_{lj} \,. \tag{2}$$

By adopting the commonly employed approximation of factorizing the V and T on-shell amplitudes out of the intermediate integrals, the above equation reduces to a simple algebraic one

$$T = (1 - VG)^{-1} V \,, \tag{3}$$

where G is a diagonal matrix containing the meson–baryon loop functions

$$G_l(P) = i \int \frac{\mathrm{d}^4 q}{(2\pi)^4} \frac{2M_l}{(P-q)^2 - M_l^2 + i\epsilon} \frac{1}{q^2 - m_l^2 + i\epsilon} \,, \tag{4}$$

with M_l and m_l denoting the mass of the baryon and meson in the loop, respectively. Here, $P = p + k = (\sqrt{s}, 0)$ is the total four-momentum in the center-of-mass frame, and q is the internal meson four-momentum.

The loop function in Eq. (4) diverges logarithmically and needs to be regularized. Typically, this is done using a cut-off regularization scheme, where the integration over the spatial components is truncated at a given value $q_{\max}$, or a dimensional regularization scheme [13]. The cut-off parameter $q_{\max}$ and the so-called subtraction constants [12] for dimensional regularization are free parameters that are typically determined by fitting the model to experimental data.

Although both schemes yield similar results close to the threshold, as we move further away from it, they may lead to structures in the T-matrix that cannot be associated with any resonance or bound state. Recall that poles appear when the T-matrix diverges, *i.e.* when $\det(1 - VG) = 0$, or when $V^{-1} \sim \mathrm{Re}(G)$ if the pole is strongly coupled to a single channel (uncoupled approach). If this relation is satisfied while the potential V is positive (repulsive), a fake pole is generated, as there is no physical justification for a repulsive interaction to produce a resonance or bound state.

In Fig. 2, we show the typical behavior of the real part of the loop function in the dimensional (G^{DR}) and cut-off (G^{CO}) regularization schemes. As observed, $\mathrm{Re}(G^{\mathrm{DR}})$ may become positive below the channel threshold, potentially giving rise to fake poles in that energy region. Likewise, $\mathrm{Re}(G^{\mathrm{CO}})$ may also acquire artificially large positive values and thus may generate unphysical structures. At energies where the center-of-mass momentum $q_{\mathrm{cm}} = q_{\mathrm{max}}$, $\mathrm{Re}(G^{\mathrm{CO}})$ diverges and develops a spiked structure; $\mathrm{Im}(G^{\mathrm{CO}})$ is also pathological since at this energy it abruptly drops to zero. The reason is purely mathematical: the divergence in the integrand of $\mathrm{Re}(G^{\mathrm{CO}})$ moves to the boundary and cannot be compensated by a principal-valued integration.

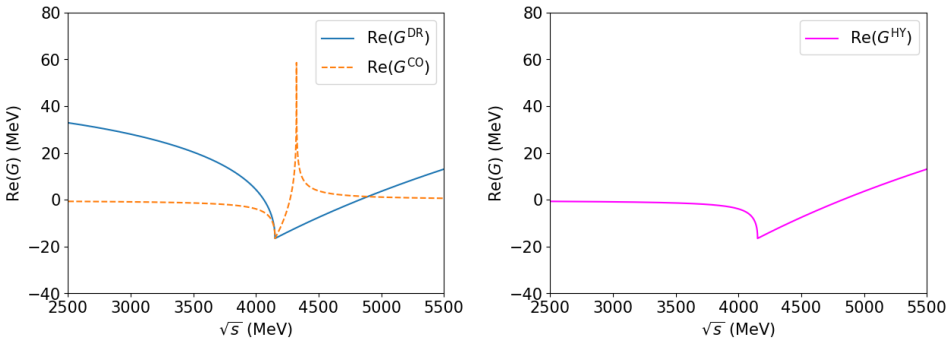

Fig. 2. (Color online) Typical behavior of the real part of the loop function in the dimensional (solid blue line), cut-off (dashed orange line), and hybrid (right panel) regularization schemes.

Consequently, for both dimensional and cut-off regularization schemes, one must check whether each dynamically generated state is genuine or fake. Such a study often requires a sophisticated analysis, and attempts to distinguish poles in a simplified, qualitative manner may be erroneous.

The novelty of our method is a hybrid loop function, $G^{\rm HY}$, that preserves only the well-behaved parts of $G^{\rm CO}$ and $G^{\rm DR}$

$$\begin{aligned} \mathrm{Re}\left(G_k^{\rm HY}(\sqrt{s}\,)\right) &= \begin{cases} \mathrm{Re}\left(G_k^{\rm CO}(\sqrt{s}\,)\right) & \text{if} \quad \sqrt{s} < M_k + m_k\,, \\ \mathrm{Re}\left(G_k^{\rm DR}(\sqrt{s}\,)\right) & \text{if} \quad \sqrt{s} \geq M_k + m_k\,, \end{cases} \\ \mathrm{Im}\left(G_k^{\rm HY}(\sqrt{s}\,)\right) &= \mathrm{Im}\left(G_k^{\rm DR}(\sqrt{s}\,)\right) \end{aligned} \tag{5}$$

subject to the condition that $\mathrm{Re}(G^{\rm CO})$ and $\mathrm{Re}(G^{\rm DR})$ match at the channel threshold. Consequently, the subtraction constants $a_k(\mu)$ are no longer independent parameters but are connected to the value of $q_{\rm max}$

$$a_k(\mu) = \frac{16\pi^2}{2M_k}\left[G^{\rm CO}k(q_{\rm max}) - G_k^{\rm DR}(\mu, a_k = 0)\right]\,. \tag{6}$$

In this work, we fix $q_{\rm max} = 600$ MeV and $\mu = 1000$ MeV.

3. New results for the $S = -1$, $I = 1$ sector

As an illustrative example, we present results for the PB interactions in the $S = -1$, $I = 1$ sector. Specifically, we shall consider the interaction of four heavy coupled channels: $\eta_c\Sigma$, $\bar{D}\Xi_c$, $\bar{D}_s\Sigma_c$, and $\bar{D}\Xi_c'$. The corresponding T-matrix is shown in Fig. 3.

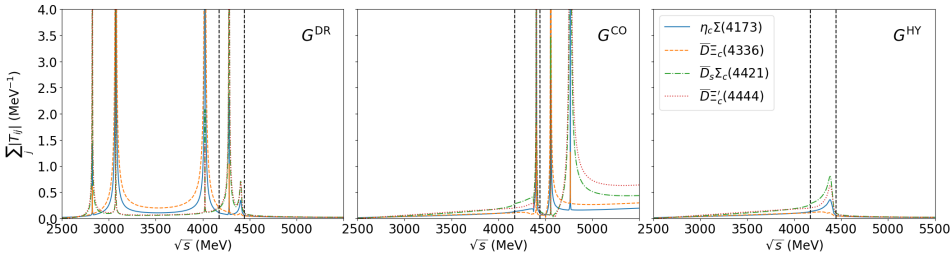

Fig. 3. (Color online) From left to right, the panels illustrate the scattering amplitude results obtained with $G^{\rm DR}$, $G^{\rm CO}$, and $G^{\rm HY}$ for the PB interaction in the $S = -1$, $I = 1$ sector. The subindex i refers to the final channel; each line represents the sum of all contributions to the $i^{\rm th}$ channel. Vertical black dashed lines indicate the thresholds of the lightest and heaviest channels.

As seen in Fig. 3, the T-matrix displays five structures when employing the $G^{\rm DR}$ loop (left panel), three structures in the case of $G^{\rm CO}$ (middle panel), and only one for $G^{\rm HY}$ (right panel). A detailed study of each of these structures allows us to discard the unphysical ones; consequently, only one

valid physical pole remains below the $\bar{D}\Xi_c'$ threshold for both the DR and CO schemes. Notably, this is the same pole obtained directly by the HY scheme, without the need for any further analysis!

Thus, the new $S = -1$, $I = 1$ PB resonance appears around 4400 MeV in all three regularization schemes. More details including results in the VB sector and for meson interaction with $(3/2^+)$ baryons are in preparation.

To summarize, our preliminary results show that the hybrid loop function method successfully eliminates unphysical artifacts in all tested strangeness and isospin sectors. Furthermore, it has revealed the existence of new pentaquarks in the $S = -1, I = 1$ sector. We hope that our work will stimulate experimental searches for these new pentaquark states, the discovery of which would significantly enrich the family of observed exotic baryons.

This work is supported by MICIU/AEI/10.13039/501100011033 through grants PID2023-147112NB-C21 and through the Maria de Maeztu Center of Excellence award to the Institute of Cosmos Sciences, grant CEX2024-001451-M.

REFERENCES

[1] LHCb Collaboration (R. Aaij *et al.*), *Phys. Rev. Lett.* **115**, 072001 (2015).
[2] LHCb Collaboration (R. Aaij *et al.*), *Phys. Rev. Lett.* **122**, 222001 (2019).
[3] LHCb Collaboration (R. Aaij *et al.*), *Sci. Bull.* **66**, 1278 (2021).
[4] LHCb Collaboration (R. Aaij *et al.*), *Phys. Rev. Lett.* **131**, 031901 (2023).
[5] Belle and Belle II collaborations (I. Adachi *et al.*), *Phys. Rev. Lett.* **135**, 041901 (2025).
[6] J. Hofmann, M.F.M. Lutz, *Nucl. Phys. A* **763**, 90 (2005).
[7] V.R. Debastiani, J.M. Dias, W.H. Liang, E. Oset, *Phys. Rev. D* **97**, 094035 (2018).
[8] J.A. Marsé-Valera, V.K. Magas, A. Ramos, *Phys. Rev. Lett.* **130**, 091903 (2023).
[9] L. Roca, J. Song, E. Oset, *Phys. Rev. D* **109**, 094005 (2024).
[10] J.A. Marsé-Valera, V.K. Magas, A. Ramos, *Phys. Rev. D* **111**, 054020 (2025).
[11] J.-J. Wu, R. Molina, E. Oset, B.S. Zou, *Phys. Rev. C* **84**, 015202 (2011).
[12] G. Montaña, A. Feijoo, A. Ramos, *Eur. Phys. J. A* **54**, 64 (2018).
[13] E. Oset, A. Ramos, C. Bennhold, *Phys. Lett. B* **527**, 99 (2002); *Erratum ibid.* **530**, 260 (2002).